Check for updates

Zhu Liangjun (Orcid ID: 0000-0003-0111-1450)

Cooper David, J. (Orcid ID: 0000-0003-3391-3538)

Li Zongshan (Orcid ID: 0000-0002-3901-945X)

Wang Xiaochun (Orcid ID: 0000-0002-8897-5077)

Regional scale temperature rather than precipitation determines vessel features in earlywood of Manchurian ash in temperate forests

L. Zhu[1, 2], D. J. Cooper[3], D. Yuan[1], Z. Li[4], Y. Zhang[5], H. Liang[6], X. Wang[1]

[1]Center for Ecological Research and Key Laboratory of Sustainable Forest Ecosystem Management-Ministry of Education, School of Forestry, Northeast Forestry University, Harbin 150040, China

[2]National Engineering Laboratory for Applied Technology of Forestry & Ecology in South China, College of Life Science and Technology, Central South University of Forestry and Technology, Changsha 410004, China

[3]Department of Forest and Rangeland Stewardship, Colorado State University, Fort Collins, CO 80523, USA

[4]State Key Laboratory of Urban and Regional Ecology, Research Center for Eco-Environmental Sciences, Chinese Academy of Sciences, Beijing 100085, China

[5]Key Laboratory of Forest Ecology and Environment of National Forestry and Grassland Administration, Research Institute of Forest Ecology, Environment and Protection, Chinese Academy of Forestry, Beijing 100091, China

[6]South China Botanical Garden, Chinese Academy of Sciences, Guangzhou 510650, China

Corresponding author: Xiaochun Wang (wangx@nefu.edu.cn)

This article has been accepted for publication and undergone full peer review but has not been through the copyediting, typesetting, pagination and proofreading process which may lead to differences between this version and the Version of Record. Please cite this article as doi: 10.1029/2020JG005955

©2020 American Geophysical Union. All rights reserved.

Key Points:

- Temperature limits vessel features of earlywood and radial growth of Manchurian ash
- The limitation of water (drought) stress in northern dry sites increased significantly
- The climate signals recorded by ring width and vessel features were almost the same
- Rapid warming increased water conduction and carbon allocation of Manchurian ash

Accepted Article

©2020 American Geophysical Union. All rights reserved.

Abstract

The earlywood vessels (EWV) of ring-porous species are formed in the outermost tree ring to guarantee efficient water transport before bud break. At present, it is unclear which climatic factors influence the formation of EWV traits of trees in temperate forests, which limits the accuracy of predicting forest response to climate change. We investigated the EWV traits of Manchurian ash (*Fraxinus mandshurica* Rupr.) in a network of 19 sites in Northeast China. Ring width (RW) was significantly negatively correlated with vessel density (VD) and positively correlated with other EWV traits, including mean vessel area (MVA), hydraulic diameter (Dh), vessel number (VN) and total vessel area (TVA). The climate signals recorded by RW and EWV traits were consistent in almost all sites. Temperature was the most important climate factor limiting xylem formation that influences RW and EWV of Manchurian ash. The minimum temperature, especially in the previous growing season, was positively correlated with RW and EWV traits, but negatively correlated with VD at almost all sites. In the drier northern sites, temperature and moisture in non-growing season also had a positive effect on RW and EWV traits. The rapid warming around 1980 significantly promotes hydraulic efficiency (Dh, VN, MVA and TVA) and carbon assimilation (RW), which provided a potential physiological mechanisms of climate warming leading to growth increase of ring-porous broadleaf species. It is worth noting that continuous climate warming has brought great benefits to tree growth, but it also increases the risk of hydraulic failure, especially in the south.

1. Introduction

Ring-porous tree species are abundant in temperate forests around the world (Kitin and Funada 2016). Earlywood vessel (EWV) is an important anatomical feature of ring-porous trees facilitating water transport (Fonti et al. 2010; Tyree and Zimmermann 2002). Any change in the EWV features, especially the size or number of vessels, may influence the

©2020 American Geophysical Union. All rights reserved.

response of trees to climate or environmental changes (Fonti et al. 2010). The Hagen–Poiseuille law predicts that hydraulic conductivity will increase with the increase of the fourth power of the lumen diameter, and even small differences in vessel size will significantly influence the water transport efficiency (Tyree and Zimmermann 2002). Wider vessels increase hydraulic efficiency, but also increase the risk of cavitation caused by drought (McDowell et al. 2008; Tyree and Sperry 1989). Trees can increase water conductivity by increasing vessel density or changing vessel distribution to avoid the risk of cavitation (Tyree and Sperry 1989).

It is unclear which climate factors influence the EWV traits of trees in temperate forests, thus limiting the accuracy of predicting forest responses to climate change (Prislan et al. 2018). Vessel features, especially their diameter, are considered to be mainly controlled by their water supply, as the availability of water affects the turgor pressure and cell expansion (Tyree and Sperry 1989). Eckstein et al. (1977) hypothesized that the vessel diameter of deciduous trees reflects the availability of water. This hypothesis has now been confirmed by some species (Abrantes et al. 2013; Campelo et al. 2010). For example, the vessel features of Holm oak (*Quercus ilex*) in the Mediterranean region of Europe are mainly limited by spring precipitation (Campelo et al. 2010).

Other studies have suggested that climate factors limiting xylem EWV formation vary with species, region and site conditions (Cai and Tyree 2010; Castagneri et al. 2020; Martinez-Sancho et al. 2017; Pourtahmasi et al. 2011). For example, the earlywood vessel size of oak (*Quercus* spp.) could be limited by the precipitation in the spring marine climate (González and Eckstein 2003), the temperature in arid areas of the inner-alpine valley (Matisons et al. 2012; Pritzkow et al. 2016), or the riparian flood period (St and Nielsen 2000). Rita et al. (2015) found that the functional anatomical traits of European holly (*Ilex aquifolium*) in mesic sites were limited by temperature, while in drought-prone areas, they

©2020 American Geophysical Union. All rights reserved.

were mainly limited by precipitation. The changes of vessel density and diameter in tropical mangrove *Rhizophora mucronate* were related to the periodic changes between dry and rainy seasons (Verheyden et al. 2005). Precipitation did not limit the xylem and vessel development of European beech (*Fagus sylvatica*) in two temperate forest sites with similar climate (Prislan et al. 2018). Therefore, further research is needed to reveal the mechanisms of xylem formation under a series of ecological and climatic conditions. In addition, xylem anatomical features can record strong or novel climatic signals (Abrantes et al. 2013; Campelo et al. 2010; Fonti et al. 2010; Venegas-Gonzalez et al. 2015). As a proxy of dendroclimatic reconstructions of past climate, it is important to assess the robustness of the annual changes in vessel features, especially in temperate forests.

Manchurian ash (*Fraxinus mandshurica* Rupr.) is one of the most important temperate hardwood species in the mixed broadleaf-Korean pine forest in northeast China. It has extensive but discontinuous distribution in northeast China, eastern Russia, northern Japan and North Korea (Wang 2004). Manchurian ash grows on lower slopes with high soil moisture content, 30 meters high and 2 meters in diameter. It appears to be highly sensitive to climate change and may be damaged by late spring frost (Su and Lin 2003).

Dendrochronological studies have confirmed that temperature is the main factor limiting the radial growth of Manchurian ash (Cao et al. 2018; Zhu et al. 2015). RW of Manchurian ash has been widely used as a proxy for temperature reconstructions in northeast China (Zhu et al. 2015). However, previous studies were based only on tree-ring width from a single site. It is of great significance to analyze the xylem formation of Manchurian ash EWV and its response to climate change on a larger geographical scale. In order to meet this demand, we conducted a regional dendroanatomical study of earlywood vessels of Manchurian ash from a network of 19 broadleaf-Korean pine forest sites in northeast China. We aim to (i) identify the relationship between RW and EWV traits of Manchurian ash; (ii) explore the main

Accepted Article

©2020 American Geophysical Union. All rights reserved.

climatic factors affecting xylem formation (RW and EWV traits) of Manchurian ash in this region, and (iii) clarify temporal and spatial variation of the relationship between climate and tree growth (RW and EWV traits) of Manchurian ash in northeast China.

2. Materials and methods

2.1. Study area

Our study area is located at the broadleaf-Korean pine mixed forests of the Changbai and Xiaoxing'an Mountains in northeast China (40.75-49.82° N, 124.75-135° E, Figure 1). The forests are dominated by *Pinus koraiensis* and some broad-leaved tree species, including *Fraxinus mandshurica*, *Phellodendron amurense*, *Juglans mandshurica*, *Betula costata*, *Quercus mongolica* and *Tilia amurensis*. Soil in this area is mainly dark-brown forest soil (Wang et al. 2019; Zhu et al. 2018b).

The study area belongs to temperate continental climate, with summer monsoon and obvious seasonality. Humid air masses from low-latitude oceans create a relatively short, warm and rainy summer, while dry and cold continental air masses invade from high latitudes (Siberian high pressure), resulting in long, cold and dry winter. Mean annual temperature ranges from 1.1 °C to 7.1 °C, with significant monthly and seasonal heat variations (Figure 1 and Table 1). January is the coldest month with an mean temperatures of -22.6 to -12 °C, and July is the hottest month with an mean temperature of 20.0 to 23.7 °C. The total annual precipitation is 592-1093 mm, with 53%~65% in summer and 3%~5% in winter (Figure 1a and Table 1).

In the past 60 years, the minimum temperature at each weather station increased significantly ($p < 0.01$), but the total annual precipitation had no significant change except Tonghe (Figure S1, b-k).The precipitation in the north is the least and the drought is frequent. The regional climate (an average of 10 weather stations) had a similar pattern (Figure S1a).

2.2. Sampling, wood preparation and data measurement

©2020 American Geophysical Union. All rights reserved.

A total of 735 cores of Manchurian ash were collected from 19 forest sites with little human disturbance (Table S1). These sites are distributed in the whole mixed broadleaf-Korean pine forest area in northeast China. One or two cores per tree were taken from the dominant or co-dominant trees at the breast height. More than 15 trees and 30 cores were taken from one site. Cores were prepared according to traditional dendrochronological procedures and visually cross-dated using the skeleton-plot method to identify possible absent or false rings (Stokes and Smiley 1968). Tree-ring width (RW) was measured with the Velmex tree-ring measurement system (Velmex, Inc., Bloomfield, NY, USA) to the accuracy of 0.001 mm. The quality of dating and measurement was checked by COFECHA computer program (Holmes 1983).

Based on cross-dating results, six representative and undamaged cores were selected from trees of similar age from each site for EWV measurement. To avoid the effect of age on anatomical feature, trees over 80 years old were selected (Gea-Izquierdo et al. 2012; Venegas-Gonzalez et al. 2015). Sample preparation and image analysis were performed according to Fonti and Garcia-Gonzalez (2008)'s method. Cores were polished with 1200 grit sandpaper. Fill the vessel lumen with white chalk to increase contrast. Then, the cores were scanned with a high-resolution of 2400 dpi Epson Perfection V600 Photo Scanner 9 (Seiko Epson Corporation, Suwa, Japan), and the images were saved as TIFF files for measurement and analysis. Image-Pro Plus 6.0 software (Media Cybernetics, Inc., Rockville, MD 20850 USA) was used to identify and analyze the EWV feature. The images were calibrated using a scale bar before measurement. Within each tree ring, a rectangular or parallelogram was defined using the formula $RW \times l$, where RW is the ring width and l is the tangent length of each ring (Figure 2). The vessel lumen area (A) ($\geq$ 5000 μm²) was obtained in each ring of each core by combining semi-automatic detection and manual editing. The area threshold ($\geq$

Accepted Article

©2020 American Geophysical Union. All rights reserved.

5000 μm²) included more than 95% of EWV. Finally, a careful visual inspection was conducted to verify that all vessel elements were included.

The tangential width (*l*) of different rings or samples varies with the size of polished section and the inner diameter of sample core. Because the vessel number (VN) and the total vessel lumen area depend on the tangent length width (*l*), we normalized these parameters to a fixed frame with a tangential width of 5000 μm. Finally, the normalized VN, mean vessel area (MVA), vessel density (VD, percentage of vessel area per ring), total vessel lumen area (TVA) and hydraulic diameter (Dh) in each ring were calculated. Dh is an important hydraulic parameter that can directly reflect hydraulic conduction (Fonti et al. 2010). It is a hydraulically weighted diameter proportional to the Hagen–Poiseuille conductivity and thus proportional to xylem hydraulic conductivity (Sperry et al. 1994). All relevant formulas are shown in Figure 2c.

The de-trend of tree ring data can remove some non-climatic noise, but it often removes valuable climatic signals inadvertently (Carrer et al. 2015). To preserve the climate signals as much as possible, we only focused on the growth characteristics of trees with the age of more than 80 years old, and did not conduct the detrending analysis. We found no significant non-climatic trend in the vessel feature series of 19 sampling sites. We averaged the time series of RW, VN, MVA, VD, TVA and Dh in six cores at each site as a site chronology of vessel feature (Figure S2) for further analysis (Gea-Izquierdo et al. 2012).

2.3. Data analyses

We aligned each RW or EWV parameter (MVA, VN, TVA, VD and Dh) time series (n = 174) by cambium age, and plotted each time series to reveal whether the RW and EWV parameters were related to cambium age. The correlation relationships between parameters of EWV features were analyzed to judge the intimate relationship between various anatomical parameters, and then to better understand their roles in hydraulic strategy of *Fraxinus*

©2020 American Geophysical Union. All rights reserved.

mandshurica. Pearson correlation between RW and each EWV trait (pooled 19 sites) was used to assess the effect of vessel characteristics (MVA, VN, TVA and VD) on ring width (RW). Then, the direct and indirect relationships between xylem traits (MVA, VN, TVA and VD) and radial growth (RW) were studied by structural equation modeling (SEM). We assume that MVA and VN can not only directly affect RW, but also indirectly affect RW through VD and TVA (Figure 3a). We used the program 'lavaan' in R package for the SEM analysis (Rosseel 2012).

Precipitation, relative humidity, mean and minimum temperature data were collected from the nearest weather station at each sampling site (http://data.cma.cn/en; Table 1). We calculated the standardized precipitation-evapotranspiration index (SPEI, time-scale of 1 months) using monthly precipitation and temperature with SPEI software (Vicente-Serrano et al. 2010). Seasonal climate data were defined as the previous summer (Psum, previous June-August), the previous autumn (Paut, previous September- November), the previous winter (Pwin, previous December-current February), the current spring (Spr, current March-May), the current summer (Sum, current June-August), the previous growing season (PGS, previous June- October), and the previous non-growing season (PNG, previous November-current April).

We used Pearson correlation to analyze the relationship between seasonal climate covariates and the RW and each EWV parameter. According to the previous research results (Zhu 2019) and related literatures (Zhu et al. 2015; Cao et al. 2019; Gu 2018), the minimum temperature, precipitation, relative humidity and SPEI were selected to analyze the relationship between earlywood vessel characteristics and climate. Four relationships between each EWV parameter and seasonal climatic factors in 19 sample sites were compared. The correlations were defined as the significant positive correlation (Pos.*), the non-significant positive correlation (Pos.), the non-significant negative correlation (Neg.) and

©2020 American Geophysical Union. All rights reserved.

the significant negative correlation (Neg.*). Four seasons (PGS, PNG, Spr and Sum) were used to analyze the spatial variability of the growth-climate relationships in the study area.

The effect of climate factors on the annual variability of RW and EWV parameters (VN, VD, MVA, TVA and Dh) were quantitatively analyzed by multiple linear regression (MLR) analysis (package car, R version 3.5.1). Variance inflation factor (VIF) criterion was used to test the collinear of the predictors. The VIF values of all predictors used in each model were lower than 5 (Table S2), and far lower than the pathological value of 10 (Kutner et al. 2004). The MLR model is as follows:

$$y = a + b_1 * P + b_2 * Rh + b_3 * T_{min} + b_4 * SPEI \quad (1)$$

where y is each EWV parameter (RW, VD, Dh, VN, MVA and TVA), P is precipitation, Rh is relative humidity, T_{min} is minimum temperature and $SPEI$ is the standardized precipitation-evapotranspiration index. The parameter "a" is the intercept of the model, and b_1, b_2, b_3, and b_4 are the slopes of P, Rh, T_{min} and $SPEI$. The contribution of each variable was compared with that of other variables using relative importance normalized to 100%, highlighting the significant predictors ($p < 0.05$).

We carried out a 20-year moving window correlation analysis to analyze the temporal stability of the growth-climate relationship. Due to the differences in ash xylem trait between the north and south of our region (Figure S3), the average RW, EWV traits and climate in these two regions were calculated. The relationship between the xylem traits (RW, VN, VD, MVA, Dh and TVA) and seasonal climatic factors was compared between northern and southern regions by using moving correlation function analysis.

3. Results

3.1. Age-related trends and relationships of RW and EWV traits

After about 50 years of cambium age, we observed a slight decrease in RW and VN, a significant increase in VD, Dh and MVA, but no trend in TVA (Figure 4). The age-related

©2020 American Geophysical Union. All rights reserved.

trend significantly decreased or disappeared when the cambium age exceeded 50 years (transition point) (Figure 4). Interestingly, growth features such as RW and VN declined before the age of 50 and remained unchanged for decades to come. However, features such as VD, Dh and MVA that increased before 50 years old continued to increase after the transition point (Figure 4). In the 1950s and 1970s, the RW, VN and TVA declined slightly, and then these variables increased (Figure S2). VD increased first and then decreased before 1980s. There was no obvious trend in Dh and MVA (Figure S2).

RW was significantly positively correlated with MVA, Dh, VN, and TVA, and significantly negatively correlated with VD (Figure 3c). VD was significantly negatively correlated with VN and positively correlated with Dh and MVA (Figure 3c). There was also a significant positive correlation between TVA and all EWV traits (Figure 3c). The positive correlation between RW and TVA with VN was stronger than that with MVA (Figure 3c), indicating that RW and TVA depended more on the number of vessel than on the size.

The structural equation model explained 86.6% of the variance of ring width and indicated that the significant positive total effect of VN on radial growth (0.61) was strong than that of MVA (0.32) (Figure 3b). MVA had direct positive effect (0.49) and indirect negative effect (-0.17) on radial growth. VN had direct and indirect positive effects on radial growth, while VD had significant negative effect (-0.69) on radial growth.

3.2. Relationship between RW, EWV traits and climate factors

The minimum temperature, especially in the growing season of previous year, was the main factor limiting RW, MVA, VN, VD, Dh and TVA at all 19 sites (Figures 5). In most sites, VD was significantly negatively correlated with the minimum temperature in all seasons, while RW and other EWV traits were significantly positively correlated with the minimum temperature (Figure 5). The effect of minimum temperature on RW and EWV traits

©2020 American Geophysical Union. All rights reserved.

in non-growing season was weaker than in growing season, but it was still a factor limiting xylem formation (Figure 5). The effect of precipitation, relative humidity and SPEI on RW and EWV were weak, although precipitation and SPEI were positively correlated with RW, VN and TVA in some sites during non-growing season (Pwin and PNG) (Figure 5).

The results of MLR indicated that temperature, rather than precipitation, contributed most to the formation of RW and EWV (Table 3). All models can explain a significant amount of variation in RW and EWV traits (Table 3). The minimum temperature explained the maximum variance in RW (41%-72%) and VD (77%-84%) for all seasons, as well as the variances in Dh (36%-61%) and VN (56%-66%) in growing season (Psum, Paut, Sum and PGS) (Table 3). In dormant seasons (Pwin, Spr and PNG), precipitation, relative humidity or SPEI were more importance in explaining changes in Dh (35% and 40%), MVA (48% and 57%), VN (47% and 68%) and TVA (37% and 59%) (Table 3). For TVA changes, precipitation in growing season (Psum, Sum and PGS) (38%-52%) explained the maximum percentage variance.

3.3. Spatial variation in growth-climate relationships

The minimum temperature of the previous growing season had a strong significant positive (negative) effect on RW, MVA, VN, Dh and TVA (VD) of Manchurian ash at almost all sites. The spatial variation of temperature effects was not obvious, and seemed to be the weakest in the southern sites (Figure 6). Relative humidity of the previous growing season was significantly positively correlated with RW, VN and TVA at some northern sites, but significantly negatively or weakly positive correlated with these features at some southern sites. The VD of Manchurian ash was the opposite (Figure 6). There was no obvious spatial relationship between the precipitation and SPEI of the previous growing season and the RW or EWV features.

©2020 American Geophysical Union. All rights reserved.

The effect of the minimum temperature in non-growing season on RW and EWV traits was weaker than that in current growing season, but precipitation and SPEI still played a decisive role in the formation of RW and EWV (Figure 7). The minimum temperature, precipitation and SPEI of the previous growing season were significantly positively (negatively) correlated with RW, MVA, VN, Dh and TVA (VD) at most northern sites (Figure 7). The influence of relative humidity in non-growing season on RW and EWV features was weak, and there was no obvious spatial pattern (Figure 7).

The temporal pattern of the relationship between xylem characteristics and climate was consistent in the south and north regions (Figure 8). The effects of precipitation and SPEI of the previous growing season on xylem features changed from positive to negative around 1980. However, the effects of precipitation and SPEI in non-growing season changed from weak positive/negative to strong positive around 1980. There was a stable positive correlation between the minimum temperature of the previous growing season and xylem features, but the effect of the minimum temperature in non-growing season changed from positive to negative around 1980 (Figure 8).

4. Discussion

4.1. Ring width-EWV traits relationship

Our results indicate that Manchurian ash significantly changes its xylem hydraulic system in response to environmental drivers. Trees in northern sites had smaller earlywood vessels than those in southern sites (Figure S2). Vessel size (Dh or MVA) of angiosperms is generally considered to be an indicator of hydraulic efficiency and safety (Fonti et al. 2010; Tyree and Sperry 1989; Vaganov et al. 2006). Drought stress was more severe in the north due to lower annual precipitation and lower soil moisture (Wang et al. 2019; Zhu et al. 2018b). It is well known that trees growing in arid areas reduce their hydraulic efficiency and improve their hydraulic safety by producing smaller vessels (Fonti et al. 2010). Vessel

©2020 American Geophysical Union. All rights reserved.

diameter is also closely related to stem elongation (Carrer et al. 2015), which helps to explain the plastic response of vessel diameter at different sites to water conditions. Older trees with small trunk diameter and shorter height are prevalent in the arid northern sites, such as MJ and ML, resulting in fewer vessel and smaller size. In the southern region with better water and temperature conditions, the higher trees with larger circumference produce a large number of vessel and a large size.

The positive relationship between RW and VN and MVA at most sites indicate that the wide ring is often accompanied by more and larger xylem vessels. We also found a positive correlation between MVA and VN, indicating that Manchurian ash increases the number and size of vessels to maximize ring width in years of favorable growth conditions , while decreases the number and size of vessels in unfavorable years (Abrantes et al. 2013; Rita et al. 2015). This finding is different from previous studies, that is, smaller vessels are formed in suitable conditions, while fewer but wider vessels are formed under unfavorable conditions (Gea-Izquierdo et al. 2012; Martinez-Sancho et al. 2017). For example, Martinez-Sancho et al. (2017) pointed out that in xeric sites, sessile oak (*Quercus petraea*) trees produced smaller vessels with lower vulnerability to cavitation after unfavorable previous summer conditions, whereas at mesic sites during a dry spring, trees produced wider rings but less vessels. These authors noted that the xylem adaption strategy exhibited similar geographical dipoles in the Mediterranean Basin. Compared with previous studies, the contrasting xylem adaption strategies in our study may be due to differences in tree species and climate (Cai and Tyree 2010; Castagneri et al. 2020; Pourtahmasi et al. 2011). Manchurian ash is more sensitive and vulnerable to drought stress than other tree species (Duan and Sun 2019), and its growth characteristics are related to hydraulic safety. Drought stress in temperate forests in northeast China is not as severe as that in the Mediterranean. The mean EWV size is usually large or similar to other reported ring-porous species (Fonti and Garcia-Gonzalez 2008; Fonti and

©2020 American Geophysical Union. All rights reserved.

García-González 2004; Souto-Herrero et al. 2018). RW and TVA depend more on the number of vessels, probably on the number of rows of earlywood vessels than on their size (Fonti and García-González 2004).

4.2. Limiting factors in xylem formation in temperate forest

The minimum temperature, especially in previous growing season, is the main climatic factor limiting radial growth and vessel features in earlywood of Manchurian ash in the temperate forests of northeastern China. The minimum temperature of the previous growing season has a significant positive effect on ash EWV traits (negative for VD) at almost all sites. This is consistent with the fact that sugar and phytohormone produced in the previous year are the main energy sources for earlywood vessel development (Perez-de-Lis et al. 2016; Vaganov et al. 2006). Previous studies have shown that the onset of vessel enlargement in ring-porous broadleaf trees starts about one month before bud swell, and most of the earlywood vessels formation is earlier than the recovery of photosynthetic activity. This also occurs in chestnut (*Castanea sativa*) (Fonti and García-González 2004) and pedunculate oak (*Quercus robur*) (Tumajer and Treml 2016). However, the limited plant hormones and assimilates produced during this period could not meet the needs of earlywood xylogenesis. The temperature during the growing season can affect the accumulation and distribution of assimilates through photosynthesis and respiration (Fritts 1976; Vaganov et al. 2006). The strong positive correlation between temperatures of the previous growing season and the Dh, MVA, VN and TVA of ring-porous Manchurian ash may be related to the increase of assimilates promoting earlywood formation in the following year (Martinez-Sancho et al. 2017; Tumajer and Treml 2016).

At the same time, we also detected significant minimum temperature, precipitation and SPEI signals of the previous non-growing season in EWV traits at some northern sites. This indicates that both temperature and moisture during the dormant season affect vessel features

©2020 American Geophysical Union. All rights reserved.

and xylem formation, as previously reported on other ring-porous broadleaf trees (Fonti and Garcia-Gonzalez 2008; Pritzkow et al. 2016). In addition to the material and energy bases, the vitality of tree and the duration of cambial activities are also important. Manchurian ash is easily to be damaged by freezing and is easily affected by frost in late spring (Su and Lin 2003; Zhu et al. 2015). The minimum temperature in the dormant season can destroy trees through frost-induced cavitation (Gea-Izquierdo et al. 2013) or directly damage cambium and fine roots (Vaganov et al. 2006). Winter precipitation occurs mainly in snow, which can increase soil moisture that affects xylem formation (Vaganov et al. 2006). In the non-growing season, more snow will protect trees from freezing damage. In addition, winter-spring temperature (Perez-de-Lis et al. 2016; Vaganov et al. 2006), precipitation and critical temperature and precipitation thresholds (Ren et al. 2018) are key factors driving the initiation of cambium activity or xylogenesis affecting enlargement of vessel secondary walls before lignification (Fritts 1976; Vaganov et al. 2006).

Differences in sampling sites, including their microtopography and microclimate, also affect vessel features and climate sensitivity (Martinez-Sancho et al. 2017; Pourtahmasi et al. 2011). We found that the spatial variability of EWV traits of Manchurian ash in response to drought was similar to those found by Rita et al. (2015). The researchers also pointed out that European holly (*Ilex aquifolium*) in mesic sites encoded temperature signals in xylem anatomical traits, and both precipitation and temperature were recorded in drought-prone sites (Rita et al. 2015). Giagli et al. (2016) found that vessel size was mainly affected by the temperature in average precipitation years (590 mm) and soil moisture in the early summer of dry years (344 mm). In northern sites, Manchurian ash produces smaller and less earlywood vessels after a dry winter. This is contrary to trees from wetter sites (Abrantes et al. 2013; Cai and Tyree 2010; Tyree and Sperry 1989). This drought adaptation strategy allows trees to maintain more soil moisture in early summer and avoid extreme adverse water potentials in

©2020 American Geophysical Union. All rights reserved.

late summer (McDowell et al. 2008). The increased positive correlation between xylem traits and precipitation/SPEI after the 1980s may be due to the rapid warming around 1980 (Figure S1). Rapid warming accelerates evaporation, leading to more severe drought stress (Wang et al. 2019). As a result, the positive effect of precipitation/drought in the previous non-growing season has become increasingly prominent, and the positive effect of temperature has turned into a negative effect, which was also found in Yezo spruce (*Picea jezoensis*) in the same study area (Zhu et al. 2018a).

4.3. Significance of anatomical vessel climate signals

It is well known that xylem anatomical features record strong and novel ecological and environmental information (Abrantes et al. 2013; Campelo et al. 2010; Fonti et al. 2010; Venegas-Gonzalez et al. 2015). The EWV traits of ring-porous species of Manchurian ash provide a new perspective for paleoclimatic reconstruction in China. In the non-growing season, the total vessel area of Manchurian ash provides a signal of SPEI significantly stronger than the ring width (Figure 7), which can be used as a promising proxy for drought identification. However, in general, climate signals of RW and EWV traits are consistent in different sites. By combining existing research with our new findings, we can emphasize that differences in environmental conditions and microclimate at any sample site may determine the climatic representativeness of vessel features. Using the growth-climate relationship of a tree species, we can understand the climatic factors that limit the features of the vessel of this tree species. For example, moisture and drought are key climatic factors limiting tree growth and xylem vessel development in the Mediterranean region (Abrantes et al. 2013; Campelo et al. 2010; Martinez-Sancho et al. 2017) and other semi-arid/arid regions, including the Tibetan Plateau (Liang et al. 2014) and Mojave Desert (Ziaco et al. 2018). In contrast, in temperate or cold temperate forests temperature is more likely to be a key factor limiting tree growth and vessel formation (Fonti and García-González 2004; Pritzkow et al. 2016). Differences in

©2020 American Geophysical Union. All rights reserved.

sampling sites should also be taken into account. For example, vessel features at mesic or high-elevation areas are often limited by temperature, while precipitation or drought stress in xeric or low-altitude areas limits these features (Gea-Izquierdo et al. 2012; Rita et al. 2015).

The growth-climate relationship of Manchurian ash suggests that climate warming will promote water conduction features (VN, Dh, MVA and TVA) and carbon allocation (RW). This may contribute to the physiological mechanisms for the growth increase caused by climate warming in northeast China (Zhu et al. 2018b). Spatiotemporal dynamics of the relationship between growth and climate indicate that Manchurian ash is suffering from severe winter drought stress after rapid warming. If climate warming continues, trees are at risk of falling or dying from hydraulic failure, especially in the south areas. Forest management processes, such as artificial precipitation during droughts, can be considered to protect Manchurian ash forests and regulate forest carbon emissions. This highlights the spatiotemporal variations of dendroclimatic relationship between xylem features and climate, which must be considered in process based growth prediction and other eco-physiological models. Combined with dendrochronology, phenology, microclimatology, ecological stoichiometry, wood anatomy, and long-term synchronous monitoring of the ecophysiology and development of main tree organs is helpful to reveal the driving mechanism of xylem formation (Steppe et al. 2015).

5. Conclusion

Temperature rather than precipitation is the main climatic factor that limit the vessel development and xylem formation of Manchurian ash in temperate forests of northeast China. The more serious water stress at northern sites made the water availability as a secondary factor affecting the radial growth and xylem traits. The RW and the TVA are more determined by the number of vessels than by the size of vessels. The xylem traits of trees

Accepted Article

©2020 American Geophysical Union. All rights reserved.

change with age, climate and site characteristics. This may be due to a trade-off between hydraulic efficiency and safety.

In the first several decades of tree life, there are age-related trends in EWV caused by height growth, which makes it possible to exclude age-related trends. The climate signals recorded by RW and EWV traits have typically consistency and uniformity, but EWV traits still provide a new perspective for paleoclimatic reconstruction. Rapid warming has a positive effect on water transport and carbon allocation, which may explain the underlying physiological mechanisms of warming-induced growth increase and expansion of the range of broad-leaved trees in temperate forests. If climate warming continues, drought stress may become a key limiting factor for the vessel development and radial growth formation of northern sites, and the effect of temperature may change from positive to negative.

Acknowledgments

This research was supported by the National Natural Science Foundation of China (41877426), the Fundamental Research Funds for the Central Universities (2572017DG02) and the Key Project of the China National Key Research and Development Program (2016YFA0600800). We thank X. Zhang and W. Song for technical assistance during the fieldwork. We are also grateful to the staff of the sampled Forestry Bureaus for their assistance in the field. The authors declare no conflict of interest from their affiliations or funding.

Data accessibility

Climate data including monthly precipitation, relative humidity, mean and minimum temperature can download from China Meteorological Data Service Center (http://data.cma.cn/en). All the ring width and earlywood vessel data can be freely obtained from ResearchGate

©2020 American Geophysical Union. All rights reserved.

(https://www.researchgate.net/publication/344360595_Zhu_et_al_2020_JGR-Biogeosciences_Supplemental_data, DOI: 10.13140/RG.2.2.17346.81600).

References

Abrantes, J., F. Campelo, I. Garcia-Gonzalez and C. Nabais. 2013. Environmental control of vessel traits in *Quercus ilex* under Mediterranean climate: relating xylem anatomy to function. Trees-Structure and Function. 27:655-662.

Cai, J. and M.T. Tyree. 2010. The impact of vessel size on vulnerability curves: data and models for within‐species variability in saplings of aspen, *Populus tremuloides* Michx. Plant, Cell & Environment 33:1059-1069.

Campelo, F., C. Nabais, E. Gutiérrez, H. Freitas and I. García-González. 2010. Vessel features of *Quercus ilex* L. growing under Mediterranean climate have a better climatic signal than tree-ring width. Trees-Structure and Function. 24:463-470.

Cao, J., B. Zhao, L. Gao, J. Li, Z. Li and X. Zhao. 2018. Increasing temperature sensitivity caused by climate warming, evidence from Northeastern China. Dendrochronologia. 51:101-111.

Carrer, M., G. von Arx, D. Castagneri and G. Petit. 2015. Distilling allometric and environmental information from time series of conduit size: the standardization issue and its relationship to tree hydraulic architecture. Tree Physiology. 35:27-33.

Castagneri, D., M. Carrer, L. Regev and E. Boaretto. 2020. Precipitation variability differently affects radial growth, xylem traits and ring porosity of three Mediterranean oak species at xeric and mesic sites. Science of the Total Environment. 699:134285.

Duan, R. and H. Sun. 2019. Evaluation on Drought Tolerance of the Major Tree Species in the Eastern Mountain Region of Northeast China. Acta Botanica Boreali-Occidentalia Sinica. 39:156-163.

©2020 American Geophysical Union. All rights reserved.

Eckstein, D., E. Frisse and F. Quiehl. 1977. Holzanatomische Untersuchungen zum Nachweis anthropogener Einflusse auf die Umweltbedingungen einer Rotbuche. Angewandte Botanik. 51

Fonti, P. and I. Garcia-Gonzalez. 2008. Earlywood vessel size of oak as a potential proxy for spring precipitation in mesic sites. Journal of Biogeography. 35:2249-2257.

Fonti, P. and I. García-González. 2004. Suitability of chestnut earlywood vessel chronologies for ecological studies. New Phytologist. 163:77-86.

Fonti, P., G. von Arx, I. Garcia-Gonzalez, B. Eilmann, U. Sass-Klaassen, H. Gaertner and D. Eckstein. 2010. Studying global change through investigation of the plastic responses of xylem anatomy in tree rings. New Phytologist. 185:42-53.

Fritts, H. 1976. Tree rings and climate. Elsevier, Amsterdam, Netherlands.

Gea-Izquierdo, G., G. Battipaglia, H. Gärtner and P. Cherubini. 2013. Xylem adjustment in *Erica Arborea* to temperature and moisture availability in contrasting climates. IAWA Journal. 34:109-126.

Gea-Izquierdo, G., P. Fonti, P. Cherubini, D. Martín-Benito, H. Chaar and I. Cañellas. 2012. Xylem hydraulic adjustment and growth response of *Quercus canariensis* Willd. to climatic variability. Tree Physiology. 32:401-413.

Giagli, K., J. Gričar, H. Vavrčík, L. Menšík and V. Gryc. 2016. The effects of drought on wood formation in *Fagus Sylvatica* during two contrasting years. IAWA Journal. 37:332-348.

González, I.G. and D. Eckstein. 2003. Climatic signal of earlywood vessels of oak on a maritime site. Tree Physiology. 23:497-504.

Holmes, R.L. 1983. Computer-assisted quality control in tree-ring dating and measurement. Tree-Ring Bulletin. 43:69-78.

Accepted Article

©2020 American Geophysical Union. All rights reserved.

Accepted Article

Kitin, P.B. and R. Funada. 2016. Earlywood vessels in ring-porous trees become functional for water transport after bud burst and before the maturation of the current-year leaves. IAWA Journal. 37:315-331.

Kutner, M.H., C. Nachtsheim and J. Neter. 2004. Applied linear regression models. McGraw-Hill Irwin.

Liang, E., B. Dawadi, N. Pederson and D. Eckstein. 2014. Is the growth of birch at the upper timberline in the Himalayas limited by moisture or by temperature? Ecology. 95:2453-2465.

Martinez-Sancho, E., I. Dorado-Linan, I. Heinrich, G. Helle and A. Menzel. 2017. Xylem adjustment of sessile oak at its southern distribution limits. Tree Physiology. 37:903-914.

Matisons, R., D. Elferts and G. Brūmelis. 2012. Changes in climatic signals of English oak tree-ring width and cross-section area of earlywood vessels in Latvia during the period 1900-2009. Forest Ecology and Management. 279:34-44.

McDowell, N., W.T. Pockman, C.D. Allen, D.D. Breshears, N. Cobb, T. Kolb, J. Plaut, J. Sperry, A. West and D.G. Williams. 2008. Mechanisms of plant survival and mortality during drought: why do some plants survive while others succumb to drought? New phytologist. 178:719-739.

Perez-de-Lis, G., S. Rossi, R. Ana Vazquez-Ruiz, V. Rozas and I. Garcia-Gonzalez. 2016. Do changes in spring phenology affect earlywood vessels? Perspective from the xylogenesis monitoring of two sympatric ring-porous oaks. New Phytologist. 209:521-530.

Pourtahmasi, K., N. Lotfiomran, A. Bräuning and D. Parsapajouh. 2011. Tree-ring width and vessel characteristics of oriental beech (*Fagus orientalis*) along an altitudinal gradient in the Caspian forests, northern Iran. IAWA Journal. 32:461-473.

©2020 American Geophysical Union. All rights reserved.

Prislan, P., K. Cufar, M. De Luis and J. Gricar. 2018. Precipitation is not limiting for xylem formation dynamics and vessel development in European beech from two temperate forest sites. Tree Physiology. 38:186-197.

Pritzkow, C., T. Wazny, K.U. Heussner, M. Slowinski, A. Bieber, I. Dorado Linan, G. Helle and I. Heinrich. 2016. Minimum winter temperature reconstruction from average earlywood vessel area of European oak (*Quercus robur*) in N-Poland. Palaeogeography Palaeoclimatology Palaeoecology. 449:520-530.

Ren, P., R. Sergio, C.J. Julio, A.M. Ellison, E. Liang and J. Penuelas. 2018. Critical temperature and precipitation thresholds for the onset of xylogenesis of *Juniperus przewalskii* in a semi-arid area of the north-eastern Tibetan Plateau. Annals of Botany. 121:617-624.

Rita, A., P. Cherubini, S. Leonardi, L. Todaro and M. Borghetti. 2015. Functional adjustments of xylem anatomy to climatic variability: insights from long-term *Ilex aquifolium* tree-ring series. Tree Physiology. 35:817-828.

Rosseel, Y. 2012. lavaan: An R Package for Structural Equation Modeling. Journal of Statistical Software. 48:1-36.

Souto-Herrero, M., V. Rozas and I. Garcia-Gonzalez. 2018. Earlywood vessels and latewood width explain the role of climate on wood formation of *Quercus pyrenaica* Willd. across the Atlantic-Mediterranean boundary in NW Iberia. Forest Ecology and Management. 425:126-137.

Sperry, J.S., K.L. Nichols, J.E. Sullivan and S.E. Eastlack. 1994. Xylem embolism in ring - porous, diffuse - porous, and coniferous trees of northern Utah and interior Alaska. Ecology. 75:1736-1752.

St, G.S. and E.J.G. Nielsen. 2000. Signatures of high-magnitude 19th-century floods in *Quercus macrocarpa* tree rings along the Red River, Manitoba, Canada. 28:899.

©2020 American Geophysical Union. All rights reserved.

Accepted Article

Steppe, K., F. Sterck and A. Deslauriers. 2015. Diel growth dynamics in tree stems: linking anatomy and ecophysiology. Trends in Plant Science. 20:335-343.

Stokes, M.A. and T.L. Smiley. 1968. An introduction to tree-ring dating. University of Chicago Press, Chicago,. xiv, 73 p. p.

Su, H. and D. Lin. 2003. Influence of main site factors on *Fraxinus mandshurica* (Oleaceae) plantation. Journal of Forestry Research. 14:83-86.

Tumajer, J. and V. Treml. 2016. Response of floodplain pedunculate oak *(Quercus robur* L.) tree-ring width and vessel anatomy to climatic trends and extreme hydroclimatic events. Forest Ecology and Management. 379:185-194.

Tyree, M.T. and J.S. Sperry. 1989. Vulnerability of xylem to cavitation and embolism. Annual review of plant biology. 40:19-36.

Tyree, M.T. and M.H. Zimmermann. 2002. Hydraulic architecture of whole plants and plant performance. *In* Xylem structure and the ascent of sap. Springer, Berlin, Heidelberg, pp 175-214.

Vaganov, E.A., M.K. Hughes and A.V. Shashkin. 2006. Environmental control of xylem differentiation. Springer, Berlin, Heidelberg.

Venegas-Gonzalez, A., G. von Arx, M.P. Chagas and M. Tomazello Filho. 2015. Plasticity in xylem anatomical traits of two tropical species in response to intra-seasonal climate variability. Trees-Structure and Function. 29:423-435.

Verheyden, A., F. De Ridder, N. Schmitz, H. Beeckman and N. Koedam. 2005. High‐resolution time series of vessel density in Kenyan mangrove trees reveal a link with climate. New Phytologist. 167:425-435.

Vicente-Serrano, S.M., S. Beguería and J.I. López-Moreno. 2010. A multiscalar drought index sensitive to global warming: the standardized precipitation evapotranspiration index. Journal of climate. 23:1696-1718.

©2020 American Geophysical Union. All rights reserved.

Wang, S. 2004. China species red list. Higher Education Press, Beijing.

Wang, X., N. Pederson, Z. Chen, K. Lawton, C. Zhu and S. Han. 2019. Recent rising temperatures drive younger and southern Korean pine growth decline. Science of the Total Environment. 649:1105-1116.

Zhu, L. 2019. Response to climate change of vessel features and radial growth of four hardwood species from temperate forests of Northeast China. Northeast Forestry University, Harbin.

Zhu, L., D.J. Cooper, J. Yang, X. Zhang and X. Wang. 2018a. Rapid warming induces the contrasting growth of Yezo spruce (*Picea jezoensis* var. *microsperma*) at two elevation gradient sites of northeast China. Dendrochronologia. 50:52-63.

Zhu, L., S. Li and X. Wang. 2015. Tree-ring reconstruction of February-March mean minimum temperature back to 1790 AD in Yichun, Northeast China. Quaternary Science. 35:1175-1184.

Zhu, L., X. Wang, N. Pederson, Z. Chen, D.J. Cooper, Y. Zhang and Z. Li. 2018b. Spatial variability in growth-climate relationships of Amur cork tree (*Phellodendron amurense*) and their connections with PDO in Northeast China. Journal of Geophysical Research-Biogeosciences. 123:1625-1636.

Ziaco, E., C. Truettner, F. Biondi and S. Bullock. 2018. Moisture-driven xylogenesis in *Pinus ponderosa* from a mojave desert mountain reveals high phenological plasticity. Plant, Cell & Environment. 41:823-836.

Accepted Article

©2020 American Geophysical Union. All rights reserved.

Table 1. Location and characteristics of weather stations nearest each sample site.

Weather station	Sample site	Long. (°E)	Lat. (°N)	Alt. (m)	MAT (°C)	MAP (mm)	Time span
Yichun	LS, WY	128.917	47.733	240.9	1.13	644.5	1956-2016
Hegang	ZX	130.267	47.333	227.9	3.35	628.9	1956-2016
Tieli	TS	128.017	46.983	210.5	1.81	636.3	1958-2016
Yilan	TH	129.583	48.267	100.1	3.62	551.9	1959-2016
Tonghe	FZ	128.733	45.967	108.6	2.65	586.5	1953-2016
Hulin	MJ, YX	132.967	45.767	100.2	3.44	581.2	1957-2016
Dunhua	DHJ, DHX, DHY, LBS	128.200	43.550	524.9	3.28	622.6	1953-2016
Songjiang	CBS, HS, LSH, XF	128.250	42.533	591.4	2.90	679.9	1958-2016
Huanren	JC, LTD	125.350	41.283	245.5	6.74	846.4	1953-2014
Kuandian	BSL	124.783	40.717	260.1	7.05	1092.5	1954-2016

Note: MAT = mean annual temperature, MAP = mean annual precipitation.

.

Accepted Article

©2020 American Geophysical Union. All rights reserved.

Table 2. Standardized path coefficients of the effects of xylem traits on radial growth.

	MVA	VN	VD	TVA
Direct effect	0.49**	0.47**	-0.69**	0.06**
Indirect effect	-0.17**	0.14**	0	0
Total effect	0.32**	0.61**	-0.69**	0.06**

Notes: MVA = mean vessel area, VN = vessel number, VD = vessel density, TVA = total vessel area. ** $p < 0.05$

Accepted Article

©2020 American Geophysical Union. All rights reserved.

Table 3. Relative importance or simultaneous effects of P, Rh, T_{min} and SPEI for each season on RW and EWV traits and R^2 of the MLR models.

		Psum	Paut	PWin	Spr	Sum	PGS	PNG
RW	P	0.20**	0.18*	0.20*	0.06	0.19**	0.23**	0.12
	Rh	0.08	0.09	0.35**	0.15*	0.07	0.07	0.23*
	T_{min}	**0.67****	0.68**	0.41**	0.72**	0.70**	0.66**	0.53**
	SPEI	0.05**	0.04	0.05	0.07**	0.04*	0.04*	0.13**
	Multiple R^2	0.13***	0.11***	0.05***	0.10***	0.13***	0.14***	0.07***
VD	P	0.14**	0.09	0.02	0.05**	0.13**	0.14**	0.06**
	Rh	0.05	0.05	0.14	0.08	0.04	0.05	0.10
	T_{min}	**0.77****	**0.84****	**0.83****	**0.80****	**0.80****	**0.80****	**0.79****
	SPEI	0.04**	0.03	0.01	0.07**	0.02	0.02	0.05**
	Multiple R^2	0.26***	0.19***	0.08***	0.21***	0.26***	0.26***	0.13***
Dh	P	0.13**	0.21**	0.32**	**0.40****	0.14**	0.19**	**0.40****
	Rh	0.20**	0.25**	**0.35****	0.15**	0.18**	0.16**	0.22**
	T_{min}	**0.60****	**0.36****	0.22**	0.29**	**0.61****	**0.51****	0.27**
	SPEI	0.07**	0.18**	0.12**	0.16**	0.08**	0.14**	0.11**
	Multiple R^2	0.12***	0.11***	0.11***	0.12***	0.12***	0.14***	0.15***
MVA	P	0.32**	**0.31****	**0.48****	**0.54****	0.31**	**0.36****	**0.57****
	Rh	0.14**	0.23**	0.28**	0.13**	0.13**	0.12**	0.16**
	T_{min}	**0.38****	0.19**	0.07**	0.12**	**0.39****	0.32**	0.12**
	SPEI	0.16**	0.28**	0.17**	0.22**	0.17**	0.20**	0.15**
	Multiple R^2	0.13***	0.09***	0.13***	0.14***	0.14***	0.16***	0.17***
VN	P	0.26**	0.13**	0.26**	0.29**	0.27**	0.22**	0.35**
	Rh	0.02	0.08	0.04	0.02	0.03	0.02	0.03
	T_{min}	**0.59****	**0.56****	0.02	0.22**	**0.58****	**0.66****	0.05**
	SPEI	0.13**	0.23**	**0.68****	**0.47****	0.12**	0.10**	**0.57****
	Multiple R^2	0.08***	0.02***	0.02***	0.05***	0.08***	0.07***	0.07***
TVA	P	**0.48****	0.05	0.32	0.10	**0.52****	**0.38****	0.13*
	Rh	0.14**	0.46**	0.26**	**0.50****	0.13**	0.21**	0.20**
	T_{min}	0.23**	**0.47****	0.05	0.24**	0.21**	0.35**	0.09**
	SPEI	0.15**	0.02	**0.37****	0.16*	0.14**	0.07**	**0.59****
	Multiple R^2	0.11***	0.02***	0.03***	0.04***	0.11***	0.09***	0.05***

Note: RW = ring width, VD = vessel density, Dh = hydraulic diameter, MVA = mean vessel area, VN = vessel number, TVA = total vessel area. P = precipitation, Rh = relative humidity, T_{min} = minimum temperature, SPEI = Standardized Precipitation Evapotranspiration Index. Psum = Summer of the previous year, Paut = Autumn of the previous year, Pwin = Winter of the previous year, Spr = Spring, Sum = Summer, PGS = the growing season of the previous year, PNG = the non-growing season of the previous year. Coefficients of each MLR model are in Table S3. Bold figures represent the climatic factor with the highest relative importance or simultaneous effects. Significance code, * p <0.05, ** p <0.01, *** p <0.001.

Accepted Article

©2020 American Geophysical Union. All rights reserved.

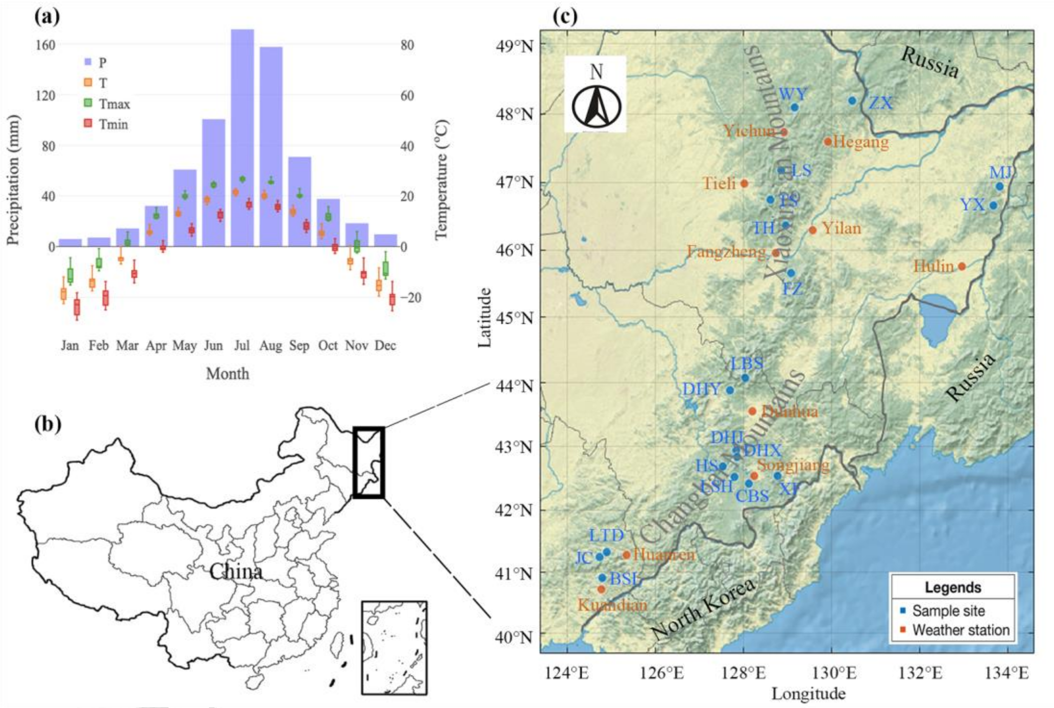

Figure 1. (a) Climate diagram for 10 weather stations for 1959-2016. (b, c) The distribution of sample sites and weather stations in study area. In figure a, blue bars represent mean monthly precipitation and color boxplots are monthly mean (T), maximum (T_{max}) and minimum (T_{min}) temperatures. In figure b, the blue and red dots represent the sampling sites and weather stations.

Accepted

©2020 American Geophysical Union. All rights reserved.

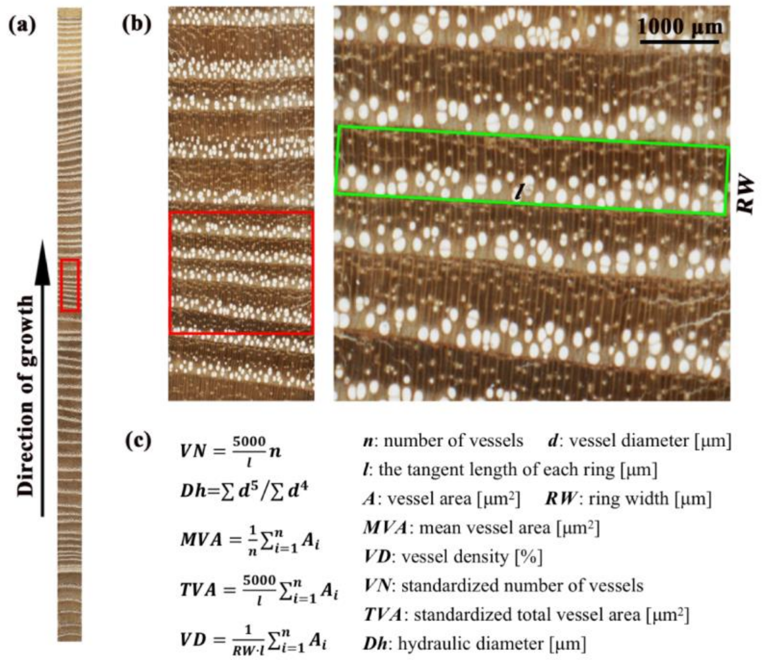

Figure 2. (a, b) Schematic illustration of tree rings xylem anatomy in Manchurian ash and (c) the definition and formula for calculating each parameter. The ring width (RW), vessel area (*A*) and the number of vessels (*n*) were measured and counted in the target area (green rectangle *l* in panel (b)) of each ring. The vessel diameter (*d*) was calculated based on the perimeter, assuming a circular lumen shape. The standardized vessel number (VN), mean vessel area (MVA), vessel density (VD), hydraulic diameter (Dh) and standardized total vessel area (TVA) were calculated for each sample. A fixed frame with a tangential width of 5000 μm was used to standardize VN and TVA.

©2020 American Geophysical Union. All rights reserved.

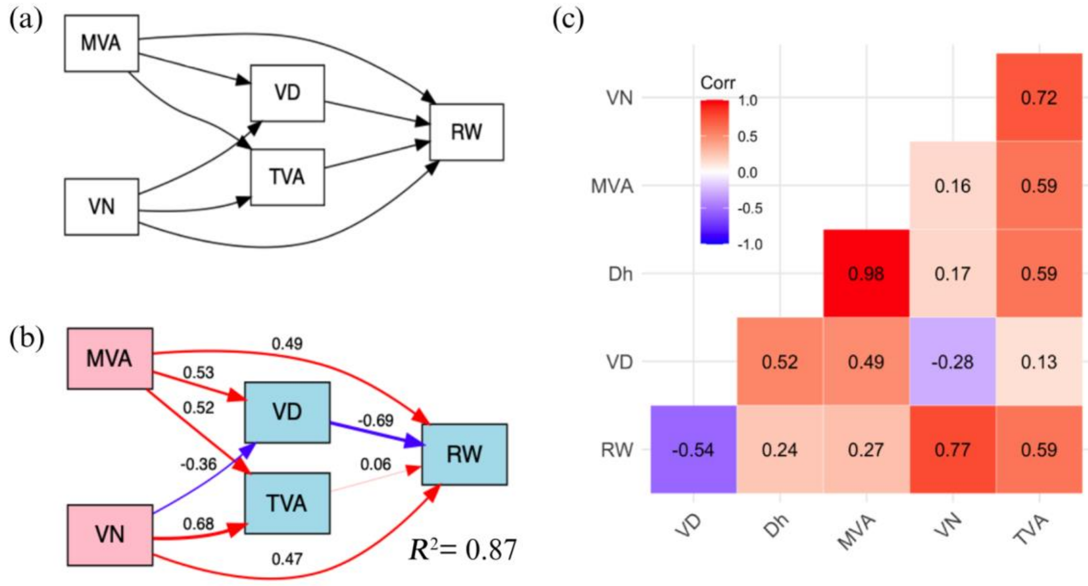

Figure 3. (a) Logical diagram of structural equation model of the interaction between xylem traits and radial grow, (b) structural equation model of effects of xylem features on radial grow of Manchurian ash, and (c) correlation relationships between RW and EWV traits. Data used in the figure is pooled by all sites. All correlation coefficients listed in figure 3a are statistically significant (p<0.05). The values in figure 3b are the standardized path coefficients representing expected change in one variable as a function of change in another in SD units. The arrow thickness is proportional to strength of path coefficients. RW = ring width, MVA = mean vessel area, VN = number of vessels, TVA = total vessel area, VD = vessel density, Dh = hydraulic diameter.

Accepted

©2020 American Geophysical Union. All rights reserved.

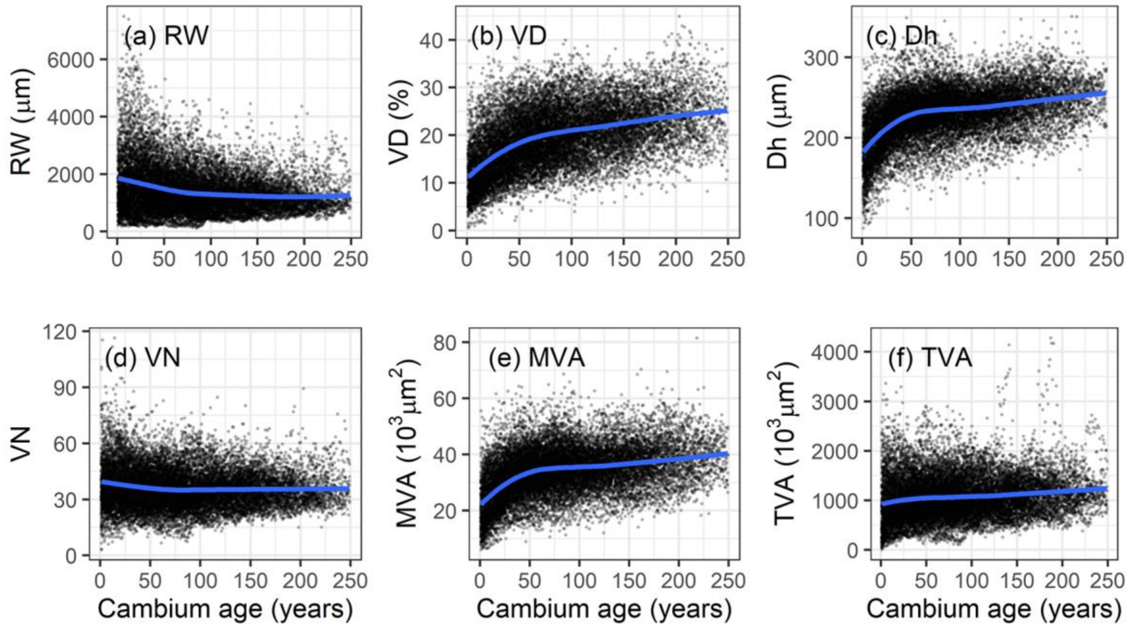

Figure 4. Trends in RW and EWV traits for all 174 trees from 19 sites. The solid blue line represents a fitted polynomial function. Data with the cambium age ≥250 years were not shown due to a significant decrease in sample depth. Cambium ages used in this work are at breast height (-1.3 m), and the age loss from the ground surface to sampling height was not considered. (a) RW-ring width, (b) VD-vessel density, (c) Dh-hydraulic diameter, (d) MVA-mean vessel area, (e) VN-vessel number and (f) TVA-total vessel area.

©2020 American Geophysical Union. All rights reserved.

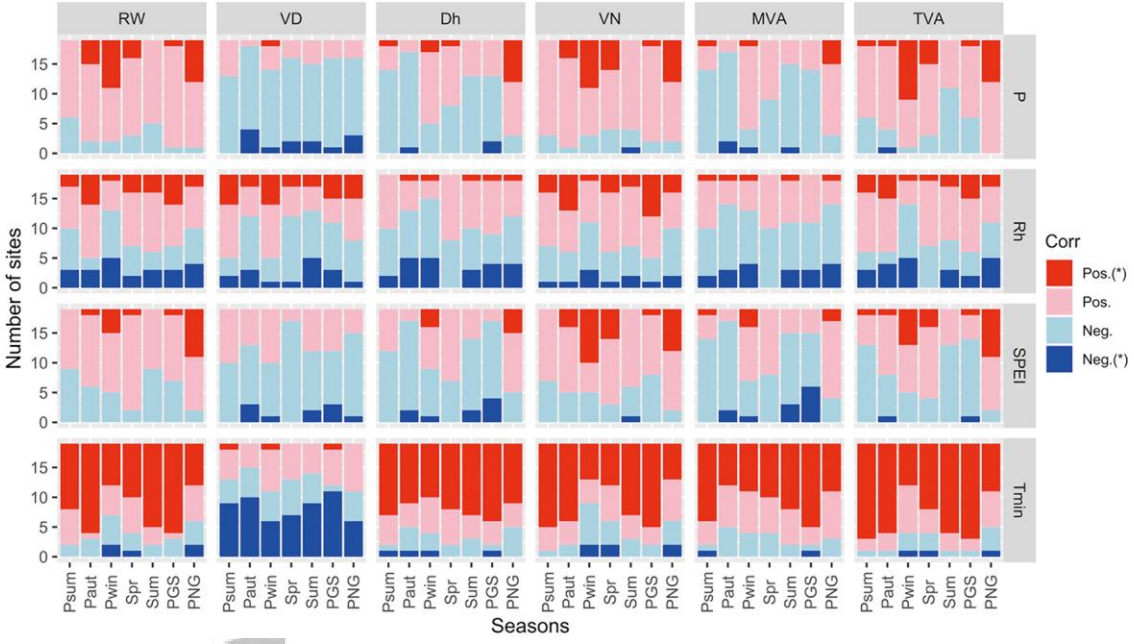

Figure 5. Number of positive and negative correlations between xylem characteristics and the major climatic factors for all 19 sites. RW-ring width, VD-vessel density, Dh-hydraulic diameter, MVA-mean vessel area, VN-vessel number, TVA-total vessel area. P = precipitation, Rh = relative humidity, T_{min} = minimum temperature, SPEI = Standardized Precipitation Evapotranspiration Index. Psum = Summer of the previous year, Paut = Autumn of the previous year, Pwin = Winter of the previous year, Spr = Spring, Sum-Summer, PGS = the growing season of the previous year, PNG = the non-growing season of the previous year. Pos.(*) = significant positive correlation, Pos = nonsignificant positive correlation, Neg. = nonsignificant positive correlation, Neg.(*) = significant positive correlation.

Accepted

©2020 American Geophysical Union. All rights reserved.

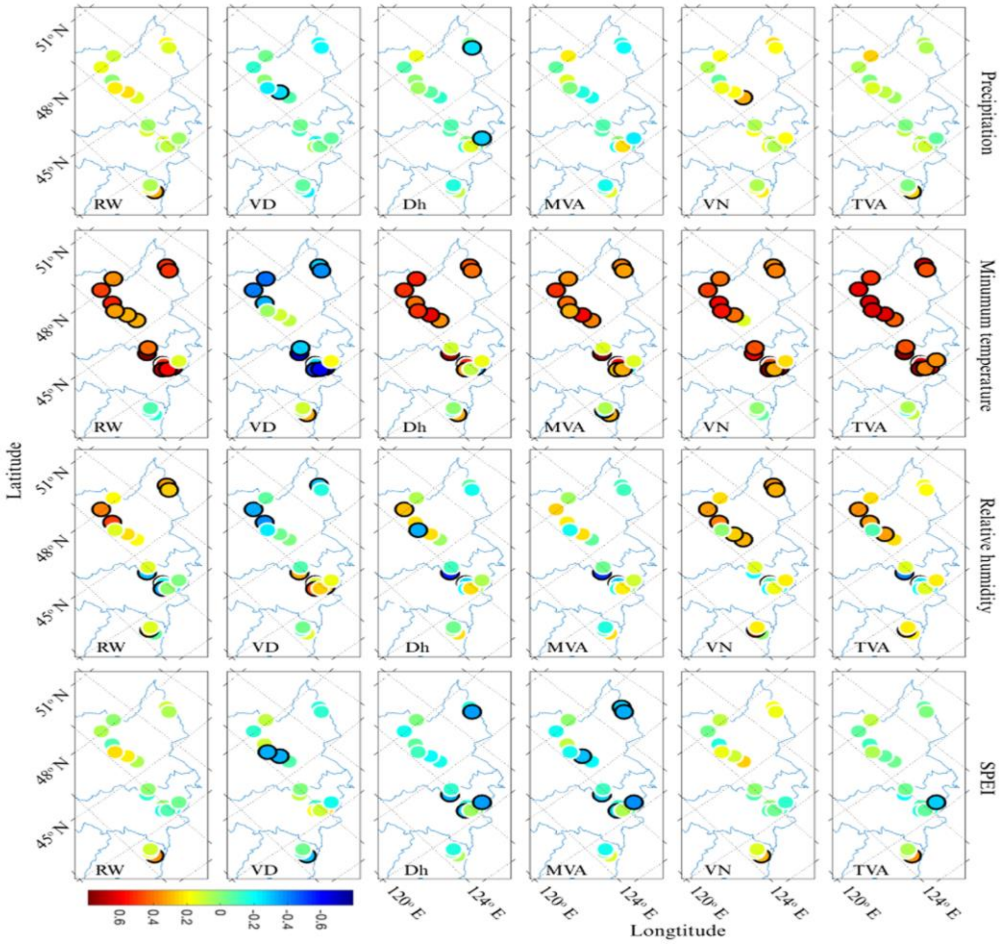

Figure 6. Relationships between the RW and EWV traits of Manchurian ash and (a) precipitation, (b) minimum temperature, (c) relative humidity and (d) SPEI in the previous growing season (PGS: P5-P10). P = precipitation, Rh = relative humidity, T_{min} = minimum temperature, SPEI = Standardized Precipitation Evapotranspiration Index. RW = ring width, VD = vessel density, Dh = hydraulic diameter, MVA = mean vessel area, VN = vessel number and TVA = total vessel area. Colors represent Pearson's correlation coefficients. Positive (negative) coefficients are represented by red (blue) colors, and circles with a black border are significant at $p = 0.05$.

Accepted

©2020 American Geophysical Union. All rights reserved.

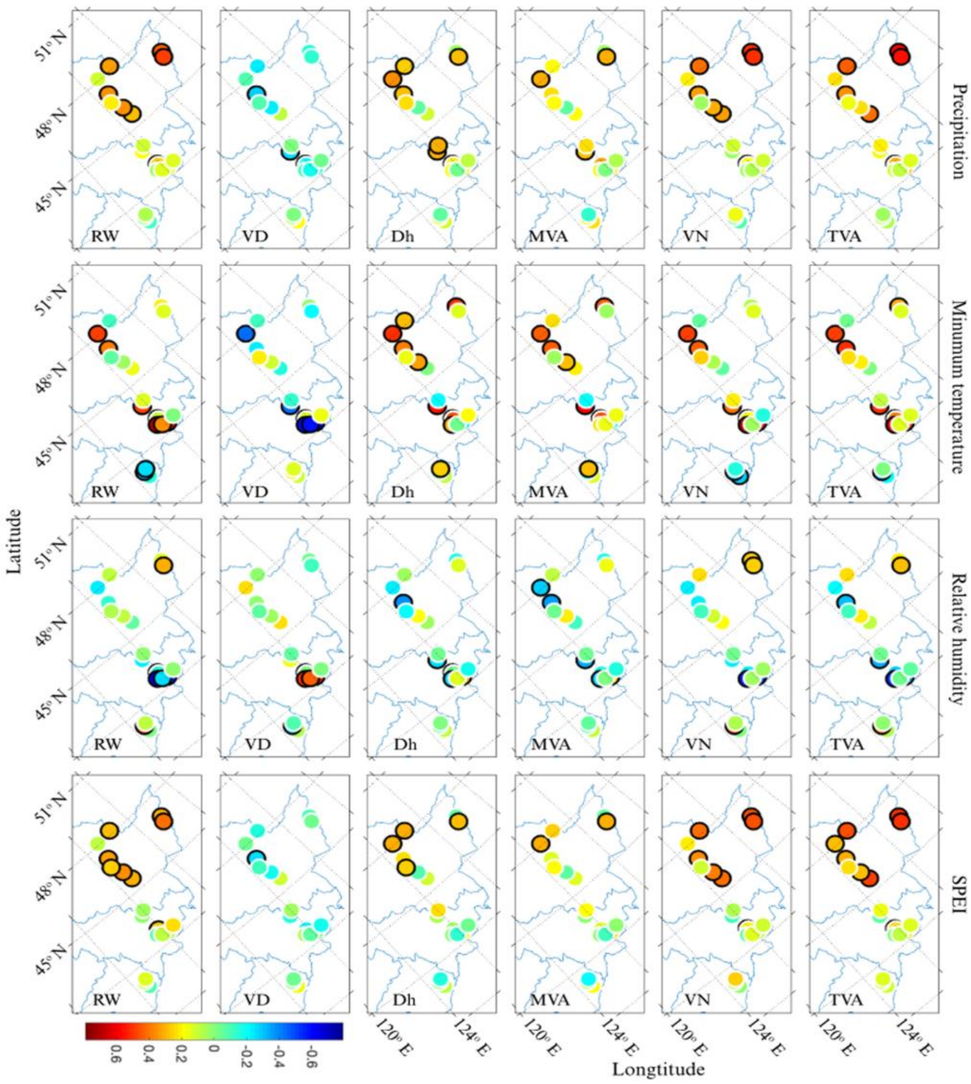

Figure 7. Relationships between the main xylem traits of Manchurian ash and (a) precipitation, (b) minimum temperature, (c) relative humidity and (d) SPEI in the non-growing season (P11-C4) of the previous year. RW = ring width, VD = vessel density, Dh = hydraulic diameter, MVA = mean vessel area, VN = vessel number and TVA = total vessel area. Colors represent Pearson's correlation coefficients. Positive (negative) coefficients are represented by red (blue) colors, and circles with a black border are significant at $p = 0.05$.

©2020 American Geophysical Union. All rights reserved.

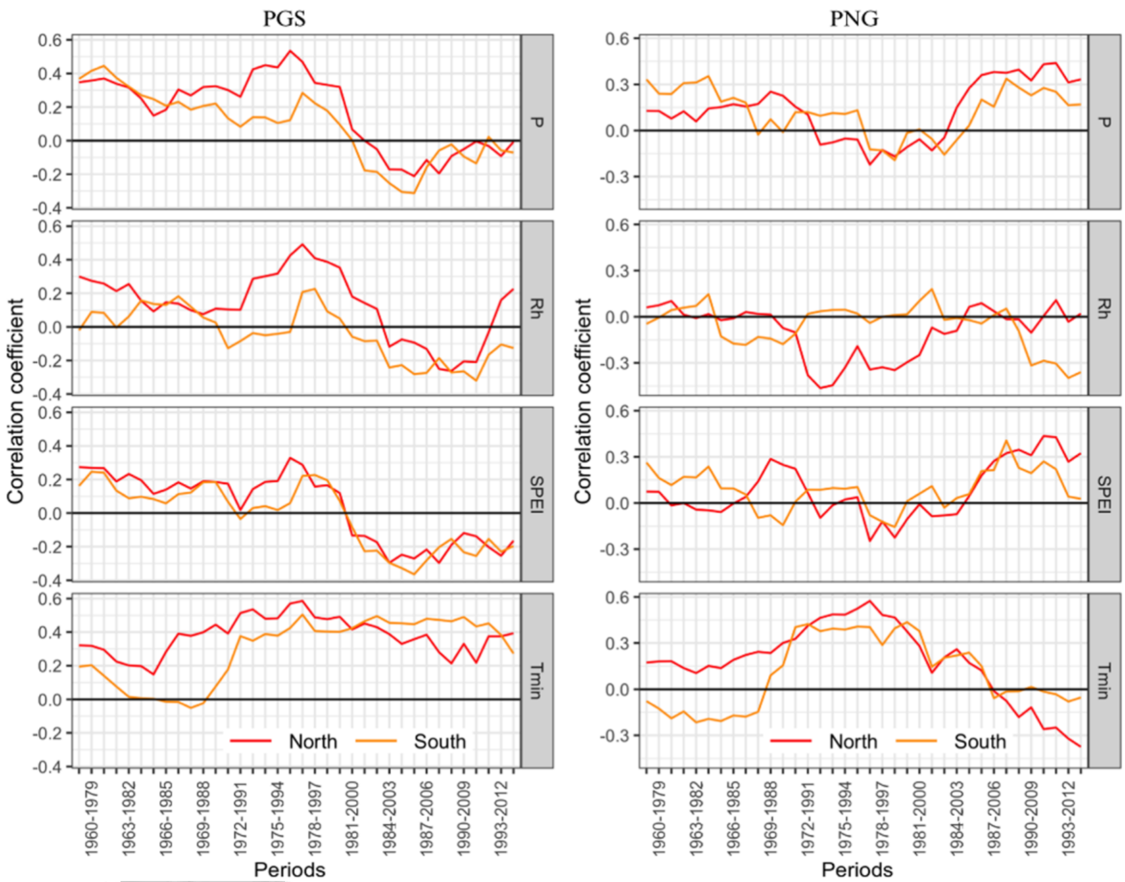

Figure 8. Mean moving correlation coefficients for xylem traits and main climate factors in the previous growing season (PGS: left panel) and non-growing season (PNG: right panel). We averaged the moving correlation coefficients of RW, Dh, MVA, VN and TVA due to their similar temporal pattern (Figure S4). VD was not considered in this analysis because it was contrary to other traits.

Accepted

©2020 American Geophysical Union. All rights reserved.